Imperial College London

Imperial College London

Department of Earth Science and Engineering

MSc in Applied Computational Science and Engineering

Independent Research Project
Final Report

Isolated skyrmion state stability exploration using mean-field models

by

Sijia Chen

Email: sijia.chen21@imperial.ac.uk
GitHub username: acse-sc121
Repository: https://github.com/ese-msc-2021/irp-sc121

Supervisors:

Dr Marijan Beg
Dr Swapneel Amit Pathak

September 2022

Abstract

Related research has shown that topologically stable skyrmions can be used as new materials for the development of data storage and information processing devices. This project aims to search the isolated skyrmion state stability which at the lowest energy states of the system using mean-field model considering temperature parameter in oder to explore the thermal and magnetic stability of the skyrmion. The material parameters of a thin-film helical magnetic FeGe nanostructure has been used to simulate a continuous three-dimensional magnetisation vector field. The exchange, zeeman and Dzyaloshinskii–Moriya energy terms are introduced in the system, and the formula of the effective field, energy density and energy for each term are implemented. We implement mean-field model and explain the detailed algorithm, it changes the entire magnetisation at once, which changes the magnitude and direction of the entire magnetisation at once, reducing computational costs and increasing the efficiency of the system. We show that the isolated skyrmion states exist at non-zero temperature, and the skyrmion number first increases and then decreases for the ideal skyrmion configuration of -1 as β increases. The critical β value for the existence of skyrmions decreases as the external magnetic field increases. Furthermore, the demagnetization energy term can be added to enhance the stability of the system.

Keywords: Micromagnetisation, Skyrmion, Mean-Field Model, Effective Field, Zeeman, Exchange, Dzyaloshinskii–Moriya.

Acknowledgements

I would like to express my sincere gratitude to my supervisor Dr Marijan Beg whose guidance and explanations helped me to overcome many difficult points and regain confidence during the project. His willingness to give his time and support so generously has been very much appreciated. I also acknowledge the support from my group memebers: Zonghui Liu and Yang Bai, who have helped me a great deal in the implementation of this study with their ideas as we have worked together over the past three months.

Moreover, I also want to thank my friends, my boyfriend and family to give me hope and always there for me in the tough times.

Contents

1 Introduction

1.1 Background and Motivation

The growing demand for data storage requires that storage technologies and materials continue to be researched and developed. Magnetic storage is the most economical data storage method [1], among which thin-film magnetic materials are widely used in hard disk drives, and their thickness are usually less than 1 micron. Relevant research showed that topologically stable magnetic skyrmions can be used as new materials to develop data storage and information processing devices. Skyrmions were first introduced to describe local particle-like configurations in field theory [2, 3], and have recently been highly correlated with spin structures in condensed matter systems. The structure can be regarded as the distribution of spin directions around a unit sphere and this texture is the result of chiral interactions [4, 5]. One possible configuration in two-dimensional is shown in Figure. 1. They can be easily manipulated using very small spin-polarized currents [6, 7], are in the nanometer-scale shapes and can be stabilized easily. Skyrmions therefore have the potential to enable new types of high-density, energy-efficient storage and logic devices [8, 9, 10, 11, 12].

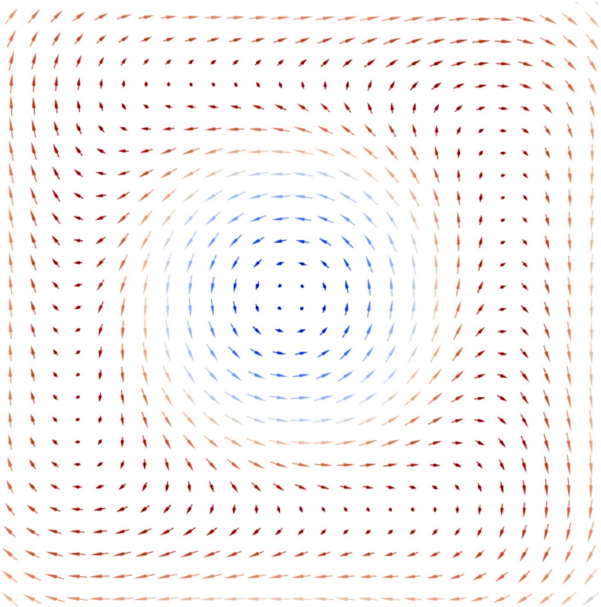

Figure 1: Two-dimensional chiral skyrmion configuration: can be regarded as the distribution of spin directions around a unit sphere.

The main challenge in the development of skyrmion-based devices has been their thermal and magnetic stability [13]. In order realize efficient data storage using skyrmions, we need to explore the range of temperatures and magnetic fields in which skyrmions exist. In addition, the thickness and diameter of thin-film materials have an effect on skyrmion stability [8]. Therefore, it is particularly important to explore the effects of temperature, external magnetic field and hosting nanostructure size on the existence of skyrmions.

1.2 Literature Review

There are two distinct spin textures in the helical magnet: helical and skyrmion [14] which can be transformed. The research [9] used a novel magnetic material, $\mathrm{Fe}_{1-x}\mathrm{Co}_x\mathrm{Si}$ [15], and explored their field and temperature dependence in details by applying an external magnetic field normal to the thin film and changing the environmental temperature. It demonstrated the region where the skyrmion appeared in the experimental and simulated phase diagrams. Taking the temperature of $25\,\mathrm{K}$ as an example, skyrmions start to appear when a weak magnetic field of $20\,\mathrm{mT}$ was applied, then completely replaced helical at $50\,\mathrm{mT}$, and the material demagnetized when the field strength increases to $80\,\mathrm{mT}$ [9]. Notably, the results showed there are no skyrmions exist in the zero magnetic field, which makes the application of disk storage more difficult.

To explore the zero-field stability of skyrmions textures, this study [8] focuses on the dependence of skyrmions on disk size and magnetic field strength. It simulated nanostructured thin-film helical magnetic FeGe disks of different thicknesses and diameters, and obtains a diameter-magnetic field (d-B) plane phase diagram by applying a magnetic field perpendicular to the thin film to observe the spin texture. It proved that skyrmionics can exist in zero-field with disk diameter $d > 140\,\mathrm{nm}$, and importantly, in the absence of an external magnetic field and without magnetocrystalline anisotropy, skyrmionic textures are the lowest energy state in the helicalmagnetic thin-film nanostructures [8]. This study did not take temperature into account ($T = 0\,\mathrm{K}$), the effect of temperature can continue to be discussed.

1.3 Objective

As demonstrated above, temperature, magnetic field and nanostructure size have effects on the existence of skyrmions, and in order for topologically stable magnetic skyrmions to be better used in data storage and information processing devices, we need to further explore their properties and characteristics. This project is proposed based on the above researches and focuses on the temperature and magnetic field dependence of skyrmions in the magnetic space of a certain size and we only consider the isolated skyrmion states (only one skyrmion exists).

The objectives of the study are listed as follows,

1) Initialisation of a continuous magnetic field $\mathbf{M}$ consisting of magnetic moments.
2) Skyrmions exist when the system is under lowest energy magnetisation state. We need to minimize three energy terms: zeeman energy, exchange energy and Dzyaloshinskii–Moriya energy.
3) Implement mean-field approximation in this project to identify the final minimal states.
4) Simulation of a three-dimensional square magnetic field to observe the existance of skyrmions by changing β and external magnetic field $\mu_0 H$.

2 Methodology

2.1 Micromagnetic System

We studied the three-dimensional continuous vector field $\mathbf{M}$ instead of atomic magnetic moments in this study. It is a function relevant to space and time, which is $\mathbf{M}(\mathbf{r},t)$. It can be thought of as a continuous magnetisation field consisting of many magnetic moments of the same cell size. The magnitude of the field is defined as M_S, it is constant and can be changed by space and time when the magnetisation field is updated. In this case, we know that $\mathbf{M} = M_\mathrm{S}\mathbf{m}$, where $\mathbf{m}$ is an unit vector. An open source Ubermag [16] package was used to initialize the system:

1) Define a square magnetisation field of size $150 \times 150 \times 30\,\mathrm{nm}^3$, the size at which the isolated state is stable and significant [8].

2) Define each cell size as $2.5 \times 2.5 \times 2.5\,\mathrm{nm}^3$, which produces more accurate results than $5 \times 5 \times 5\,\mathrm{nm}^3$.

3) Assigning values to magnetic moments.

2.2 Magnetic energies

In magnetic systems, the magnetic skyrmion configuration we discussed depends on three interactions: exchange energy, zeeman energy and Dzyaloshinskii–Moriya energy. The exchange energy is for interactions between two neighbour magnetic moments $\boldsymbol{\mu}_i$ and $\boldsymbol{\mu}_j$, which is $-J\boldsymbol{\mu}_i \cdot \boldsymbol{\mu}_j$, we assume the exchange constant $J > 0$ [17] in this project. The neighbouring moments tend to be parallel when the exchange energy is minimal, but they have no preferred direction, whereas zeeman energy does. Zeeman energy only depends on the external magnetic field $\mathbf{B}$ of each magnetic moments $\boldsymbol{\mu}$, which is $-\boldsymbol{\mu} \cdot \mathbf{B}$ [17]. The spins should in the same direction to the external magnetic field $\mathbf{B}$ in order to minimize the energy. The most important interaction for skyrmion configuration is the Dzyaloshinskii–Moriya (DMI) energy, which is a short range interaction comes from interface. It has two different types determines by the different materials: bulk DMI and interfacial DMI, and we mainly discuss bulk DMI in this project. It can be calculated by $-\mathbf{D} \cdot (\boldsymbol{\mu}_i \times \boldsymbol{\mu}_j)$, where $\mathbf{D}$ is the Dzyaloshinskii vector [18, 19]. It tends to align neighbouring magnetic moments vertically. We computes the effective field, magnetic energy density and energy of these energy terms in this project which should be used in the mean-field model discussed in Section. 2.3.

Effective field is an approximate theory which equates the effect of energy on the magnetic moments to the effect of an external magnetic field, which can be defined as,

$$\mathbf{H}_\mathrm{eff} = \frac{1}{\mu_0}\mathbf{B}_\mathrm{eff} = \frac{1}{\mu_0}\left(-\frac{\delta E[\mathbf{m}]}{\delta \mathbf{M}}\right) = -\frac{1}{\mu_0 M_\mathrm{s}}\frac{\delta E[\mathbf{m}]}{\delta \mathbf{m}}. \tag{1}$$

Magnetic energy density can be calculated by,

$$w = -\frac{\mu_0 M_\mathrm{S}}{2}\mathbf{m} \cdot \mathbf{H}_\mathrm{eff}. \tag{2}$$

And total energy of each energy term can be calculated using value of density,

$$E = \int_V w \, \mathrm{d}V, \tag{3}$$

where $\mathrm{d}V$ can be computed as $\mathrm{d}x\mathrm{d}y\mathrm{d}z$.

The detailed methods of each energy term have been discussed in the following sections.

2.2.1 Symmetric exchange energy

$$\mathbf{H}_{\mathrm{eff}}^{\mathrm{ex}} = \frac{2A}{\mu_0 M_{\mathrm{S}}} \nabla^2 \mathbf{m}, \tag{4}$$

where $\nabla^2\mathbf{m}$ is the laplace operator of unit vector field $\mathbf{m}$, A is the exchange energy constant.

Second order central difference has been used to calculate the results of laplace operator, which is

$$\begin{aligned} \nabla^2 \mathbf{m} &= \frac{\partial^2 \mathbf{m}}{\partial x^2} + \frac{\partial^2 \mathbf{m}}{\partial y^2} + \frac{\partial^2 \mathbf{m}}{\partial z^2} \\ &= \frac{\mathbf{m}(x+\mathrm{d}x) + \mathbf{m}(x-\mathrm{d}x) - 2\mathbf{m}(x)}{\mathrm{d}x^2} \\ &+ \frac{\mathbf{m}(y+\mathrm{d}y) + \mathbf{m}(y-\mathrm{d}y) - 2\mathbf{m}(y)}{\mathrm{d}y^2} \\ &+ \frac{\mathbf{m}(z+\mathrm{d}z) + \mathbf{m}(z-\mathrm{d}z) - 2\mathbf{m}(z)}{\mathrm{d}z^2}. \end{aligned} \tag{5}$$

In order to calculate the entire field, the system should be padded with ghost layers. Neumann boundary condition has been applied for exchange energy term, which means that items of ghost layers are exactly same as the boundary items, which can be expressed as $\frac{\mathrm{d}\mathbf{m}}{\mathrm{d}\mathbf{n}} = 0$.

2.2.2 Zeeman energy

$$\mathbf{H}_{\mathrm{eff}}^{\mathrm{z}} = \mathbf{H} = \frac{1}{\mu_0}\mathbf{B}, \tag{6}$$

where $\mathbf{B}$ is the external magnetic field strength, the shape of the effective field should be same as magnetisation vector field. It is worth mentioning that the coefficients of zeeman's magnetic energy density is quite different with other energy terms, which should be,

$$w = -\mu_0 M_{\mathrm{S}} \mathbf{m} \cdot \mathbf{H}_{\mathrm{eff}}^{\mathrm{z}}. \tag{7}$$

2.2.3 Dzyaloshinskii-Moriya energy

$$\mathbf{H}_{\mathrm{eff}}^{\mathrm{dmi}} = -\frac{2D}{\mu_0 M_{\mathrm{S}}} \nabla \times \mathbf{m}, \tag{8}$$

where $\nabla \times \mathbf{m}$ is the curl of unit vector field $\mathbf{m}$, D is the DMI material scalar parameter.

$$\nabla \times \mathbf{m} = \left(\frac{\partial \mathbf{m}_z}{\partial y} - \frac{\partial \mathbf{m}_y}{\partial z}\right)\hat{\boldsymbol{\imath}} + \left(\frac{\partial \mathbf{m}_x}{\partial z} - \frac{\partial \mathbf{m}_z}{\partial x}\right)\hat{} + \left(\frac{\partial \mathbf{m}_y}{\partial x} - \frac{\partial \mathbf{m}_x}{\partial y}\right)\hat{\boldsymbol{k}} = \begin{bmatrix} \frac{\partial \mathbf{m}_z}{\partial y} - \frac{\partial \mathbf{m}_y}{\partial z} \\ \frac{\partial \mathbf{m}_x}{\partial z} - \frac{\partial \mathbf{m}_z}{\partial x} \\ \frac{\partial \mathbf{m}_y}{\partial x} - \frac{\partial \mathbf{m}_x}{\partial y} \end{bmatrix} \tag{9}$$

First order central difference has been used to calculate the results of curl, which is,

$$\frac{\partial \mathbf{m}}{\partial \mathbf{n}} = \frac{\mathbf{m}(\mathbf{n} + \mathrm{d}\mathbf{n}) - \mathbf{m}(\mathbf{n} - \mathrm{d}\mathbf{n})}{2\mathrm{d}\mathbf{n}} \tag{10}$$

Dirichlet boundary condition has been used to calculate curl of $\mathbf{m}$, which means the items of ghost layers have been thought as zero vectors. This conclusion is derived from a comparison with the results of Ubermag [16], where the DMI effective field results calculated using this boundary condition are identical to those of Ubermag [16].

2.3 Mean-field model

Mean-field model has been used in this project to minimize the energy of the field, which can updated the entire field at once. The algorithm of mean-field model has been listed as follows,

Algorithm 1 Mean-Field Algorithm

1: Calculate effective field of current magnetisation vector field $\mathbf{M}_{\mathsf{old}}$: $\mathbf{H}_{\mathsf{eff}} = \mathbf{H}^{\mathsf{z}}_{\mathsf{eff}} + \mathbf{H}^{\mathsf{ex}}_{\mathsf{eff}} + \mathbf{H}^{\mathsf{dmi}}_{\mathsf{eff}}$
2: **while** current iteration $<$ 12500 iteration && tolerance $<$ 1e-4 **do**
3: Update magnitude of magnetisation $|\mathbf{M}_{\mathsf{new}}| = M_{\mathsf{S}} \cdot Langevin(\beta\mu_0|\mathbf{H}_{\mathsf{eff}}|) \cdot \frac{\mathbf{H}_{\mathsf{eff}}}{|\mathbf{H}_{\mathsf{eff}}|}$
4: Update direction of magnetisation $\mathbf{M}_\lambda = \mathbf{M}_{\mathsf{old}} + \lambda(\mathbf{M}_{\mathsf{old}} - \mathbf{M}_{\mathsf{new}})$
5: Renormalization the magnetisation $\mathbf{M}_{\mathsf{new}} = \frac{\mathbf{M}_\lambda}{|\mathbf{M}_\lambda|} \cdot |\mathbf{M}_{\mathsf{new}}|$
6: Calculate effective field of updated magnetisation $\mathbf{M}_{\mathsf{new}}$: $\mathbf{H}_{\mathsf{eff}} = \mathbf{H}^{\mathsf{z}}_{\mathsf{eff}} + \mathbf{H}^{\mathsf{ex}}_{\mathsf{eff}} + \mathbf{H}^{\mathsf{dmi}}_{\mathsf{eff}}$
7: Compare the difference $\mathbf{M}_{\mathsf{new}} - \mathbf{M}_{\mathsf{old}} =$ tolerance
8: **end while**

Output: Final state of magnetisation vector field $\mathbf{M}$ when energy is minimum.

The schematic of mean-field model has been shown in Figure.2, in which black arrows represent the magnetic moment in each cell and red arrows represent corresponding effective field. Once initialize the magnetization vector field with magnetic moments, calculate the effective field $\mathbf{H}_{\mathsf{eff}}$ of the system which has the same shape of $\mathbf{M}$. The schematic shows the steps in each iteration and the predicted final state.

Mean-field changes the magnitude and direction of the magnetisation field in each iteration. The change in magnitude of the magnetisation field is due to the introduction of β into the system, and the change in magnitude of the magnetisation field varies for different locations where the effective field is calculated. The new magnitude can be calculated using,

$$|\mathbf{M}_{\mathsf{new}}| = M_{\mathsf{S}} \cdot Langevin(\beta\mu_0|\mathbf{H}_{\mathsf{eff}}|) \cdot \frac{\mathbf{H}_{\mathsf{eff}}}{|\mathbf{H}_{\mathsf{eff}}|}, \tag{11}$$

where $Langevin(x) = \coth x - x^{-1}$ is the Langevin function.

We use the damping constant λ to determine degrees the magnetisation field should changed. In the

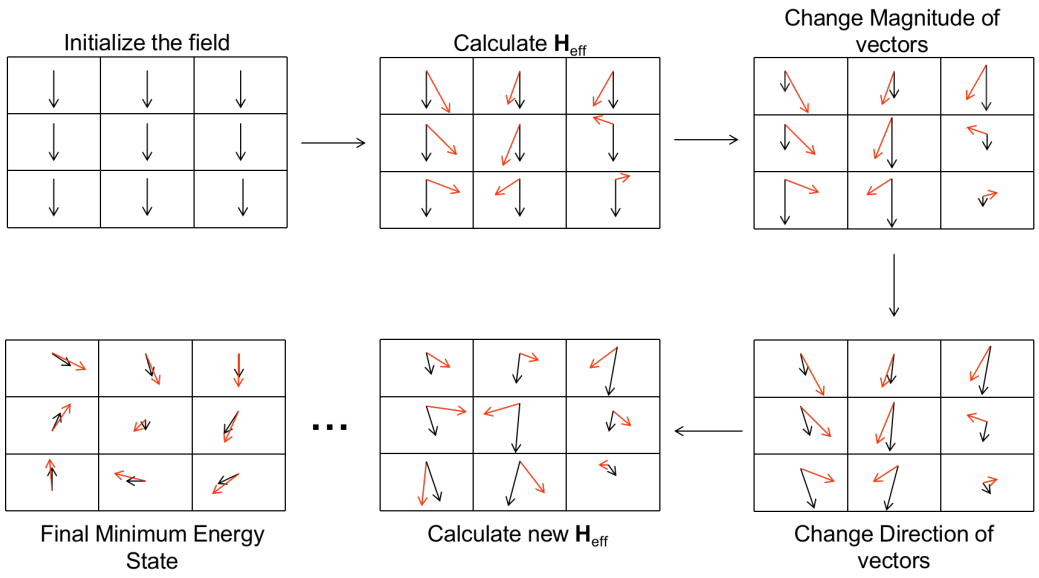

Figure 2: Mean-field Algorithm schematic: black arrows represent the magnetic moments in each cell and red arrows represent corresponding effective fields. 1. Initialize the magnetisation field with magnetic vectors; 2. Calculate effective field $\mathbf{H}_{\text{eff}}$; 3. With effect of β, calculate the new magnitude of magnetisation field; 4. With effect of effective field, calculate the new direction of magnetisation field; 5. After iterations, the total energy of the magnetisation field comes to minimal.

system, A large change in direction would result in results that would not converge, so lamda was set to a small value 0.005. The equation can be expressed as,

$$\mathbf{M}_{\text{new}} = \mathbf{M}_{\text{old}} + \lambda(\mathbf{M}_{\text{old}} - \mathbf{M}_{\text{new}}). \tag{12}$$

It is important to renormalise the new magnetisation vector field to ensure that the magnitude of the updated field is the calculated value, as the above step will affect the magnitude.

When the unit vector field approach the effective field, which is $\mathbf{m} \times \mathbf{H}_{\text{eff}} = 0$, the system energy has reached its minimum value. We use the difference between the old and new magnetisation vector fields as the stop criteria. The new magnetisation field is rotated in the direction of the effective field, and when the difference is very small, it means that the direction of the current magnetisation field is already approaches to the effective field and that the system is stabilising.

2.4 Skyrmion number and injective scalar value

In order to discuss the existence of skyrmions, the topological skyrmion number on x-y plane can be computed using skyrmion number formula:

$$S = \frac{1}{4\pi} \int \mathbf{m} \cdot \left(\frac{\partial \mathbf{m}}{\partial x} \times \frac{\partial \mathbf{m}}{\partial y} \right) \mathrm{d}x\mathrm{d}y \ [8], \tag{13}$$

where $\mathbf{m}$ is the unit magnetisation vector field of the final state. It calculates the number of times a magnetization field have covered a sphere and can characterise the direction of the magnetic moments. When the magnetisation field is in the isolated skyrmion state, S should satisfy as $S = \pm 1$.

We also define the scalar value S_{a} for two-dimensional samples are:

$$S_{\mathrm{a}} = \frac{1}{4\pi} \int \left| \mathbf{m} \cdot \left(\frac{\partial \mathbf{m}}{\partial x} \times \frac{\partial \mathbf{m}}{\partial y} \right) \right| \mathrm{d}x\mathrm{d}y \text{ [8]}, \tag{14}$$

2.5 Thermodynamic beta

One of the most important parts of this project was the incorporation of temperature into the system. We use thermodynaaic beta in the study, which defines as,

$$\beta = \frac{1}{k_B T}, \tag{15}$$

where T is the Kelvin temperature, k_B is the Boltzmann constant which is dynamic. This thermodynamic beta can be changed from 0 to infinity. It is applied in Langevin function to influence the magnitude of magnetic field. When the system is under zero temperature which is $T = 0\,\mathrm{K}$, β converges to positive infinity, result of Langevin function coverges to 1. As the temperature increases, the value of β decreases.

2.6 Material parameters

In this project we use thin-film helical magnetic FeGe square nanostructure, a popular material in skyrmion-related research with a critical temperature of $T_{\mathrm{C}} = 278.7\ \mathrm{K}$ [20], the saturation magnetisation $M_{\mathrm{S}} = 384\ \mathrm{kAm^{-1}}$, the exchange energy constant $A = 8.78\ \mathrm{pJm^{-1}}$ and the DMI material parameter D is $|D| = 1.58\ \mathrm{mJm^{-2}}$ [8]. It is worth mentioning that for this material, the uxiaxial anisotropic energy can be neglected, so this energy was not included in this study.

3 Code Metadata

The project is developed to object-oriented programming (OOP) in Python. An open source Ubermag [16] package has been used to initialize the system and test the results. The environment and dependencies are listed as follows,

1) Operating System: macOS Monterey 12.4

2) Compiler: Python 3.8

3) Dependencies:

   (a) NumPy [21]

   (b) discretisedfield [22]

   (c) micromagneticmodel [16]

   (d) oommfc [23]

   (e) Matplotlib [24]

4 Results and Analysis

4.1 Stable states at zero temperature

In order to find the state of existence of the isolated skyrmions, various possibilities of local energy minimum states need to be identified and mean-field model is applied to search for the state of minimum energy magnetisation in the constrained helicoidal magnetic nano-structures. We use the ubermag package to build a continuous three-dimensional model and calculate them by varying the environmental parameters in simulations. Initialize the system with unit vectors, define the size of each cell with $2.5 \times 2.5 \times 2.5\,\text{nm}^3$ or $5 \times 5 \times 5\,\text{nm}^3$, and a real thin-film helical FeGe square nanostructure is used to simulate with magnetisation field size is $150 \times 150 \times 30\,\text{nm}^3$. An external magnetic field perpendicular to the sample is applied to the system in the positive z-direction. The outputs of final minimal states of the field under zero temperature are shown in Figure. 3. In order to plot the states of the field, mpl function in Ubermag [16] has been used.

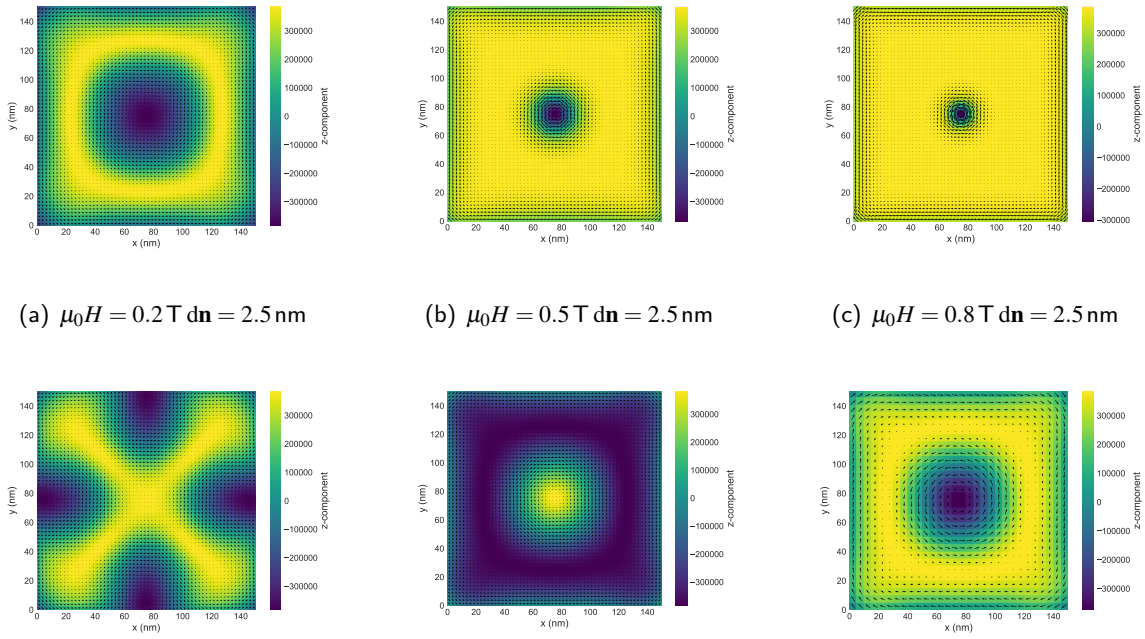

(a) $\mu_0 H = 0.2\,\text{T}$ $d\mathbf{n} = 2.5\,\text{nm}$ (b) $\mu_0 H = 0.5\,\text{T}$ $d\mathbf{n} = 2.5\,\text{nm}$ (c) $\mu_0 H = 0.8\,\text{T}$ $d\mathbf{n} = 2.5\,\text{nm}$

(d) $\mu_0 H = 0.2\,\text{T}$ $d\mathbf{n} = 2.5\,\text{nm}$ (e) $\mu_0 H = -0.2\,\text{T}$ $d\mathbf{n} = 2.5\,\text{nm}$ (f) $\mu_0 H = 0.2\,\text{T}$ $d\mathbf{n} = 5\,\text{nm}$

Figure 3: Existence of different spin textures for $\beta \to \infty$, the external magnetic field (0, 0, $\mathbf{H}$) is applied in the positive z-direction, initialize vectors with (0, 0, -1) except (d)(e) with opposite(0, 0, 1): (a) Isolated skyrmion state with $\mu_0 H = 0.2\,\text{T}$ and $2.5\,\text{nm}$ cell size. (b) Isolated skyrmion state with $\mu_0 H = 0.5\,\text{T}$ and $2.5\,\text{nm}$ cell size. (c) Isolated skyrmion state with $\mu_0 H = 0.8\,\text{T}$ and $2.5\,\text{nm}$ cell size. (d) Helical state with (0, 0, 1) initialize state, $\mu_0 H = 0.2\,\text{T}$ and $2.5\,\text{nm}$ cell size. (e) Isolated Skyrmion state of opposite configuration with $\mu_0 H = -0.2\,\text{T}$ and $2.5\,\text{nm}$ cell size. (f) Isolated skyrmion state with $\mu_0 H = 0.2\,\text{T}$ and $5\,\text{nm}$ cell size.

From Figure. 3(a) 3(b) 3(c), we can conclude that at zero temperature, the size of the skyrmion becomes smaller as the external magnetic field strengthens. According to Equation 6, we know that

the effective field and energy of the zeeman is determined by the strength of the external magnetic field. As the strength of the external magnetic field increases, the corresponding effective field of the zeeman also increases, with more influence on the overall effective field. As introduced in Section.2.2, when the energy is minimal, zeeman term tends to direct the magnetic moments in the same direction as the external magnetic field. In the simulation, the external magnetic field being applied in the positive z-direction, so that at the minimum state of the system, the magnetisation vector field tends to be oriented in the positive z-direction, implying that the stronger the external field, the larger the yellow part in the plots and the smaller the size of skyrmion.

The initialisation state of the magnetisation field vectors also affects the existence and stability of the skyrmions. As shown in Figures.3(a) and 3(d), when the initial vectors set to $(0,0,1)$, zeeman and exchange terms are under minimum energy states because all vectors in the field are exactly in the same direction as the external magnetic field and parallel to each other. Zeeman term is in a high proportion of the overall system energy, so that DMI term, which makes the vectors tend to perpendicular to each other, plays a small role, the skyrmion cannot appear.

Furthermore, as can be seen from the comparison of Figure.3(a) and 3(f), the size and stability of the skyrmions are not affected by cell size, and smaller cells have the more accurate the results. When the cell size is $5 \times 5 \times 5\,\mathrm{nm}^3$, the shape of the magnetisation field is $(30,30,6)$, while when the cell size is $2.5 \times 2.5 \times 2.5\,\mathrm{nm}^3$, the shape is $(60,60,12)$. It means that more magnetic vectors contain in the field with smaller cells, and it can be understood as the field has more samples, so that the more accurate results can be obtained.

4.2 Skyrmion number S

As mentioned in the previous section, skyrmions were shown to exist at zero temperature ($\beta \to \infty$) and the following discussion focuses on the effect of temperature and magnetic field magnitude on the skyrmions when the temperature is not zero, we use β as a parameter representing temperature in this study. In Section.2.4, skyrmion number S has been introduced to describe how many times the configurations have covered a sphere. According to the Equation 13 and using topological charge function in discretisedfield [22], the skyrmion number S and scalar value S_a can be calculated under different β and $\mu_0 H$.

The simulation takes seven sets of data with external magnetic field strengths from $0.2\,\mathrm{T}$ to $0.8\,\mathrm{T}$, decreasing β from 5300 and observing the outputs of the plots to determine the existence of the skyrmions, the results have been shown in the Figure.4. The thin-film magnetic material FeGe has been used, and the parameters are listed in the Section.2.6.

The results are proved that skyrmions can exist when temperatures are not zero, and the configurations are influenced by temperature. In Figure.4(a), the points that are connected in a line correspond to states where skyrmions exist, and they all correspond to values of the number of skyrmions S between -0.4 and -0.7. The ideal value of the skyrmion number for an isolated skyrmions is -1 (determined by chirality), but in the real case there is an error due to the magnetisation tilting at the boundary. We can observe that for each external magnetic field strength $\mu_0 H$, the number of skyrmions S increases

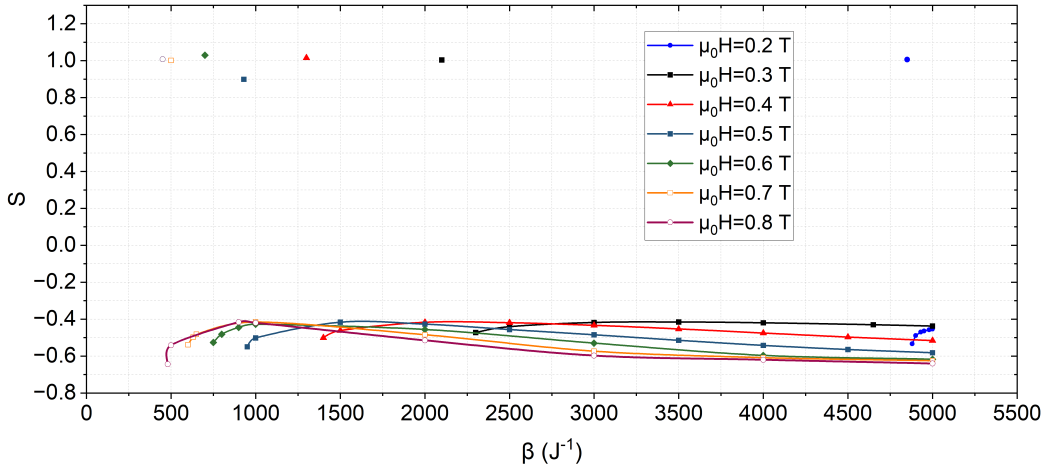

(a) β and Skyrmion number S with different external magnetic field $\mu_0 H$.

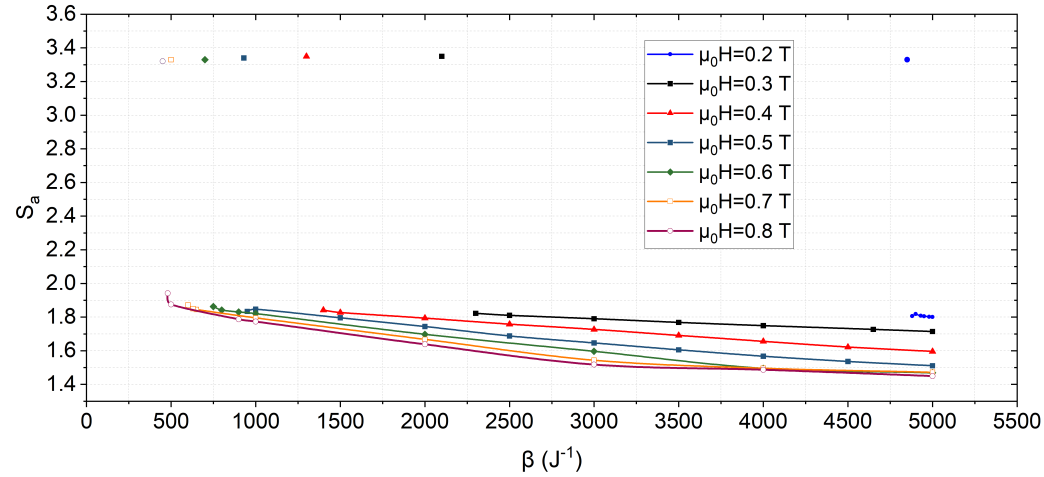

(b) β and Skyrmion scalar number S_{a} with different external magnetic field $\mu_0 H$.

Figure 4: Results of Skyrmion number with different β and $\mu_0 H$: the points that are connected in line correspond to states where skyrmions exist; the single points at the upper of the figures correspond to helical state. Seven sets of data with external magnetic field strengths from $0.2\,\text{T}$ to $0.8\,\text{T}$ were simulated. Skyrmions exist from the leftmost critical β to $\beta \to \infty$.

and then decreases as β decreases until skyrmions disappear, and that the number of skyrmions at the critical β value is similar to that at $\beta = 5300$. With small external magnetic field $\mu_0 H$, the critical β is large and the turning point can not be seen in the figure. For the small magnetic field case $\mu_0 H = 0.2\,\text{T}$, this pattern of change is not reflected because the turning point should occur at $\beta > 5300$. Helical state appears when β less than critical value, which corresponds to the points that values are approximately 1 in this case. It means that skyrmions disappear with high temperature. Figure.4(b) shows the scalar value of skyrmion number, which computes the sum with the absolute values of $(\frac{\partial \mathbf{m}}{\partial x} \times \frac{\partial \mathbf{m}}{\partial y})$, and is a positive value. The value of S_{a} increasing slowly between 1.4 and 2 as β decreases. The scalar value of helical state is greater than 3 shown in the figure. To be mentioned, it is not shown in the figure that skyrmions also exist from $\beta = 5300$ to $\beta \to \infty$, which means skyrmions

exist from zero temperature to critical β for each $\mu_0 H$.

In addition, the critical value of β decreases as the external magnetic field increases and the relationship between the two parameters is shown in the figure below. It means that skyrmions exist over a larger temperature range at a stronger external magnetic field.

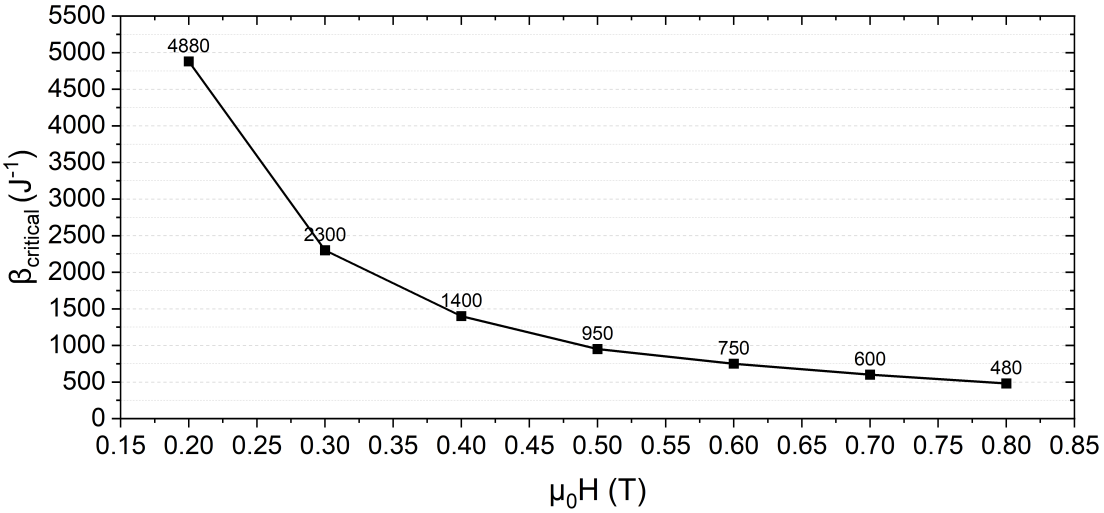

Figure 5: Relationship between critical β and external magnetic field $\mu_0 H$. Seven external magnetic fields from $0.2\,\mathrm{T}$ to $0.8\,\mathrm{T}$ intervals of $0.1\,\mathrm{T}$ were simulated. As external magnetic field increases, value of critical β decreases.

4.3 Stable states at non-zero temperature

In this section, the skyrmion configuratios under non-zero temperature will be discussed. The following figure is simulated at different β: 5000 and 2000, the applied external magnetic fields are $0.2\,\mathrm{T}$ and $0.8\,\mathrm{T}$. It can be seen that the with stronger external magnetic field, the skyrmion size becomes smaller. This output can be compared with configurations at zero temperature shown in Figure.3, the skyrmion size of Figure.6(b) is larger than Figure.3(c), which means that temperature has an effect on the size of skyrmion. The higher temperature (lower β), the more active the magnetisation field will be and the larger the change in each iteration, which might reducing the effect of the zeeman energy on the system and thus slow up the change of skyrmion configurations. According to the Figure.6(b) and 6(c), the skyrmion with lower β has a slightly larger size compared with larger β. As discussed above, the higher temperature, the magnetisation vectors more disordered, thus it is complicated for zeeman energy to reach the energy minimum state and the vertical upward (yellow) part of the magnetisation will be smaller, which may be responsible for the larger skyrmion size for lower β.

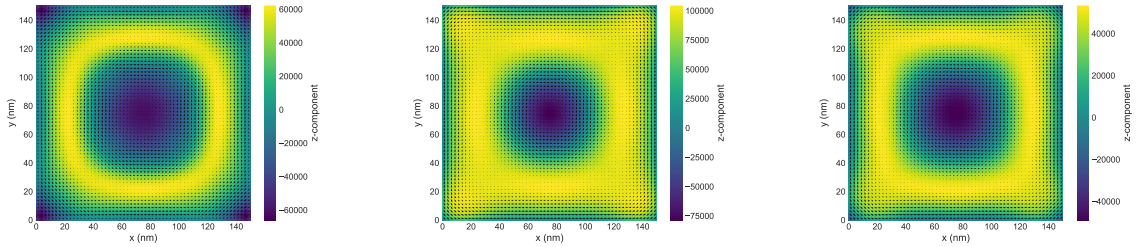

(a) $\beta = 5000$ $\mu_0 H = 0.2\,\mathrm{T}$ (b) $\beta = 5000$ $\mu_0 H = 0.8\,\mathrm{T}$ (c) $\beta = 2000$ $\mu_0 H = 0.8\,\mathrm{T}$

Figure 6: Skyrmion states at non-zero temperature. (a) $\beta = 5000$ and external magnetic field is $\mu_0 H = 0.2\,\mathrm{T}$. (b) $\beta = 5000$ and external magnetic field is $\mu_0 H = 0.8\,\mathrm{T}$. (c) $\beta = 2000$ and external magnetic field is $\mu_0 H = 0.8\,\mathrm{T}$. From(a)(c), skyrmion size decreases when external magnetic field increases, but the change is not as obvious as at zero temperature. From (b)(c), when β decreases the skyrmion size becomes larger slightly.

4.4 Performance of Mean-field Model

The mean-field model was used in the simulations, successfully identified the lowest energy states of the system and searched for skyrmion states with the addition of the temperature parameter. The stop criteria for finding the difference between the old and new magnetisation vector field allows the system to converge before the maximum iterations and the execution time is within a reasonable range. For example, when $\mu_0 = 0.7\,\mathrm{T}$ and $\beta = 3000$, the execution time for the appearance of skyrmions is 269 seconds with 5427 iterations. The longest time spent for each $\mu_0 H$ is also efficient when β at the critical state, as follows listed in the table. The results are for a magnetisation field simulation of size $150 \times 150 \times 30\,\mathrm{nm}^3$ and cell size of $2.5 \times 2.5 \times 2.5\,\mathrm{nm}^3$ and is sufficient to demonstrate the high efficiency of this approximation method: mean-field.

Table 1: Final skyrmion states of critical β for different $\mu_0 H$.

$\mu_0 H$(T)	$\beta_{\text{critical}}(\mathrm{J}^{-1})$	Initial Energy(J)	Final Energy(J)	Iteration
0.2	4880	5.18×10^{-17}	-5.76×10^{-17}	17 000
0.3	2300	7.78×10^{-17}	-6.14×10^{-17}	11 803
0.4	1400	1.04×10^{-16}	-6.12×10^{-17}	11 906
0.5	950	1.30×10^{-16}	-6.09×10^{-17}	15 000
0.6	750	1.56×10^{-16}	-6.10×10^{-17}	11 749
0.7	600	1.81×10^{-16}	-6.10×10^{-17}	11 808
0.8	480	2.07×10^{-16}	-6.14×10^{-17}	12 000

5 Discussion

5.1 Strengths and Limitations

The project aims to discover isolated skyrmion existence which is under lowest energy magnetisation state, mean-field is the most important part of this project, which can ignore the collective effects of thermal fluctuations and efficient obtain qualitative characteristics of the phase diagrams [25]. Different from the Monte-Carlo simulation with high computational cost, mean-field model uses the concept of effective field to change the state of all particles in the magnetisation field at once and in the specified directions, which greatly improves the computational efficiency and reduces the computational cost. In addition, β, as one of the parameters has been studied the properties of thermodynamic phases.

However, the accuracy of the results may be reduced because the entire field changes together, meaning that there may be some parts of the vector field that change too little or too much in one iteration, leading to errors, or failure to reach the final stable state of convergence.

5.2 Attempt

1) Landau-Lifshitz-Gilbert equation (LLG) has been tried to change the direction of magnetisation vectors in mean-field model, which is,

$$\mathbf{M}_{\text{new}} = \mathbf{M}_{\text{old}} - \alpha \mathbf{M}_{\text{old}} \times (\mathbf{M}_{\text{old}} \times \mathbf{H}_{\text{eff}}), \tag{16}$$

where α is the damping constant. Initially it was intended to omit the renormalization step which might change the direction of the vector field slightly, but by trying we found that the efficiency of this method is similar to the more intuitive λ method, so it was not adopted in the end.

2) The previous algorithm used stop condition $\mathbf{m} \times \mathbf{H}_{\text{eff}} = 0$ to stop iterating and output the final state when the maximum value of $\mathbf{m} \times \mathbf{H}_{\text{eff}}$ matrix was within the tolerance. However, we found that the system often continued to iterate after the system had already found the minimum energy state, and stopping at the set maximum iterations. This may be due to the fact that the majority of the magnetic moments in the system already met the condition, but individual moments did not and so the maximum value did not reach the set tolerance value.

5.3 Future Plan

There are four possible aspects that could be improved in the future study. Firstly, demagnetization energy can be added in the total energy terms which is generated due to the interaction of the magnetic moments, also known as dipolar interaction energy. It allows for a more uniform magnetisation system and enhances the stability of the system. The functions in discretisedfield [22] have been implemented the calculation of the demagnetisation energy term which can be added in the project by adjusting the parameters. The next point is about damping constant λ using in mean-field model to update the direction of the magnetisation field can be improved to a dynamic value just like learning rate. At the beginning of the iteration, λ can be a larger value around 0.4 to 0.6. As the iterations increases, the direction of the magnetic vectors gradually approach the direction of the effective field and λ should

decrease accordingly. It will substantially reduces the computational losses and allows the system to find the minimum energy state more efficiently and accurately. Also, the micromagnetisation system can be changed from a square to disk which are more likely to be used in magnetic storage. The boundary conditions for the disk should be considered in this case. The final suggestion would be to do simulations with more sets of data to investigate the relationship between β, external magnetic field $\mu_0 H$ and skyrmion number S, and to draw a contour plot by adding S as labels for each β and $\mu_0 H$ data point.

6 Conclusion

With implement of mean-field model, the isolated skyrmion state has been observed at both zero and non-zero temperatures. The skyrmion existence is affected by the initialization state of magnetisation and skyrmion size is significantly smaller with stronger external magnetic field under zero temperature. The value of skyrmion number S has been affected by different β and external magnetic field, which increases and then decreases with increasing β for each magnetic field, while the scalar value of it continuously declining. Also, helical state appears when β reaches a critical value, where the critical value decreases with increasing external magnetic field strength, meaning the presence of skyrmions in stronger magnetic fields over a wider temperature range. For skyrmion state at non-zero temperature, the relationship between size and external magnetic field is the same as at zero temperature, but the difference between fields is significantly smaller. In addition, in the same field, the size becomes slightly smaller for larger β. Furthermore, the computational cost of mean-field demonstrate to be low based on the small number of iterations.

References

[1] P. Grundy, "Thin film magnetic recording media," *Journal of Physics D: Applied Physics*, vol. 31, no. 21, p. 2975, 1998.

[2] T. H. R. Skyrme, "A unified field theory of mesons and baryons," *Nuclear Physics*, vol. 31, pp. 556–569, 1962.

[3] R. Rajaraman, "Solitons and instantons. 1. reprint as a paperback." pp. 115–123, 1987.

[4] A. Fert, V. Cros, and J. Sampaio, "Skyrmions on the track," *Nature nanotechnology*, vol. 8, no. 3, pp. 152–156, 2013.

[5] H. Yang, A. Thiaville, S. Rohart, A. Fert, and M. Chshiev, "Anatomy of dzyaloshinskii-moriya interaction at co/pt interfaces," *Physical review letters*, vol. 115, no. 26, p. 267210, 2015.

[6] F. Jonietz, S. Mühlbauer, C. Pfleiderer, A. Neubauer, W. Münzer, A. Bauer, T. Adams, R. Georgii, P. Böni, R. A. Duine *et al.*, "Spin transfer torques in mnsi at ultralow current densities," *Science*, vol. 330, no. 6011, pp. 1648–1651, 2010.

[7] X. Yu, N. Kanazawa, W. Zhang, T. Nagai, T. Hara, K. Kimoto, Y. Matsui, Y. Onose, and Y. Tokura, "Skyrmion flow near room temperature in an ultralow current density," *Nature communications*, vol. 3, no. 1, pp. 1–6, 2012.

[8] M. Beg, R. Carey, W. Wang, D. Cortés-Ortuño, M. Vousden, M.-A. Bisotti, M. Albert, D. Chernyshenko, O. Hovorka, R. L. Stamps *et al.*, "Ground state search, hysteretic behaviour and reversal mechanism of skyrmionic textures in confined helimagnetic nanostructures," *Scientific reports*, vol. 5, no. 1, pp. 1–14, 2015.

[9] X. Yu, Y. Onose, N. Kanazawa, J. H. Park, J. Han, Y. Matsui, N. Nagaosa, and Y. Tokura, "Real-space observation of a two-dimensional skyrmion crystal," *Nature*, vol. 465, no. 7300, pp. 901–904, 2010.

[10] X. Yu, N. Kanazawa, Y. Onose, K. Kimoto, W. Zhang, S. Ishiwata, Y. Matsui, and Y. Tokura, "Near room-temperature formation of a skyrmion crystal in thin-films of the helimagnet FeGe," *Nature materials*, vol. 10, no. 2, pp. 106–109, 2011.

[11] X. Zhang, M. Ezawa, and Y. Zhou, "Magnetic skyrmion logic gates: conversion, duplication and merging of skyrmions," *Scientific reports*, vol. 5, no. 1, pp. 1–8, 2015.

[12] N. S. Kiselev, A. Bogdanov, R. Schäfer, and U. Rößler, "Chiral skyrmions in thin magnetic films: new objects for magnetic storage technologies?" *Journal of Physics D: Applied Physics*, vol. 44, no. 39, p. 392001, 2011.

[13] Editorial, "Skyrmionics in sight," *Nature nanotechnology*, vol. 8, no. 12, p. 883, 2013.

[14] M.-G. Han, J. Garlow, Y. Kharkov, L. Camacho, R. Rov, J. Sauceda, G. Vats, K. Kisslinger, T. Kato, O. Sushkov *et al.*, "Scaling, rotation, and channeling behavior of helical and skyrmion

spin textures in thin films of te-doped Cu_2OSeO_3," *Science advances*, vol. 6, no. 13, p. eaax2138, 2020.

[15] W. Münzer, A. Neubauer, T. Adams, S. Mühlbauer, C. Franz, F. Jonietz, R. Georgii, P. Böni, B. Pedersen, M. Schmidt *et al.*, "Skyrmion lattice in the doped semiconductor $Fe_{1-x}Co_xSi$," *Physical Review B*, vol. 81, no. 4, p. 041203, 2010.

[16] M. Beg, M. Lang, and H. Fangohr, "Ubermag: Toward more effective micromagnetic workflows," *IEEE Transactions on Magnetics*, vol. 58, no. 2, pp. 1–5, 2021.

[17] S. Blundell, "Magnetism in condensed matter: oxford master series," *Condensed Matter Physics (Oxford Series Publications, 2001)*, vol. 29, 2001.

[18] I. Dzyaloshinsky, "A thermodynamic theory of "weak" ferromagnetism of antiferromagnetics," *Journal of physics and chemistry of solids*, vol. 4, no. 4, pp. 241–255, 1958.

[19] T. Moriya, "Anisotropic superexchange interaction and weak ferromagnetism," *Physical review*, vol. 120, no. 1, p. 91, 1960.

[20] B. Lebech, J. Bernhard, and T. Freltoft, "Magnetic structures of cubic FeGe studied by small-angle neutron scattering," *Journal of Physics: Condensed Matter*, vol. 1, no. 35, p. 6105, 1989.

[21] C. R. Harris, K. J. Millman, S. J. Van Der Walt, R. Gommers, P. Virtanen, D. Cournapeau, E. Wieser, J. Taylor, S. Berg, N. J. Smith *et al.*, "Array programming with numpy," *Nature*, vol. 585, no. 7825, pp. 357–362, 2020.

[22] M. Beg, M. Lang, R. A. Pepper, T. Kluyver, and H. Fangohr, "discretisedfield: Python package for definition, reading, and visualisation of finite difference fields." Nov. 2019. [Online]. Available: https://doi.org/10.5281/zenodo.3539461

[23] M. Beg, R. A. Pepper, and H. Fangohr, "User interfaces for computational science: A domain specific language for oommf embedded in python," *AIP Advances*, vol. 7, no. 5, p. 056025, 2017.

[24] J. D. Hunter, "Matplotlib: A 2d graphics environment," *Computing in science & engineering*, vol. 9, no. 03, pp. 90–95, 2007.

[25] O. Hovorka and T. J. Sluckin, "A computational mean-field model of interacting non-collinear classical spins," *arXiv preprint arXiv:2007.12777*, 2020.